JOURNAL OF AIRCRAFT
Vol. 43, No. 1, January–February 2006

High-Order Modeling and Experimental Validation of Local Effects in Sandwich Beams

Elena Bozhevolnaya*
Aalborg University, 9220 Aalborg, Denmark
and
Yeoshua Frostig†
Technion—Israel Institute of Technology, 32000 Haifa, Israel

Junctions of cores with different material properties in sandwich beams are considered. Substantial local effects arise in the vicinity of the junction when the panel is subjected to a vertical load. These effects, which can not be described in the frames of the classical sandwich theory, manifest themselves in a development of bending normal stresses in sandwich faces, as well as in a rise of the transverse normal stress and variation of the shear stress in the adjacent cores. High-order modeling applied to a beam in the three-point bending revealed a significant scale of the stresses locally induced at the core junctions in the sandwich beam compared to the expected level of global stresses. The followed experimental investigation of a representative sandwich beam fully confirmed the findings of the analytical modeling.

I. Introduction

PRACTICAL functionality of sandwich structures always requires usage of cores of various densities and mechanical properties in the same sandwich structural element. Various inserts in the form of backing plates, fully and partly potted inserts, edge stiffeners, etc., are also typical substructures[1,2] used in sandwiches. This may have a purpose to optimize the weight/cost of the sandwich structure or locally reinforce it for further rigging, joining facilities. Discrepancy of the mechanical properties at the junctions of adjoined materials in the sandwich core usually causes an inducement of local stresses at the material discontinuities under the applied loads. This may lead to a local failure of the bordering materials at the junction and in the end jeopardize the integrity of the whole sandwich structure.

A classic first-order sandwich theory[2,3] is not able to describe local effects in sandwich structures, and therefore, higher-order theories must be employed. Frostig and Baruch[4] and Frostig et al.[5] have developed such models, which take into account through-the-thickness normal stress in the sandwich core and allow dissimilar deflections of the faces. Effects of the concentrated loads and supports were successfully described with the help of this high-order theory approach,[5] which with certainty allows recounting for the local stress concentrations due to the presence of junctions of various cores in sandwich beams.

A closed-form analytical model[6] for sandwich beams with junctions of different cores has shown that rather strong singularities of the stresses may arise in the face sheets of the sandwich panel when subjected to a transverse out-of-plane loading. The followed experimental study of the local effects in the faces[7] has largely confirmed the results of the analytical modeling. The model[6] has also indicated rather strong stresses in the cores connected at the junction, although the accuracy of prediction of core stresses was rather low. On the whole, the nature of the local effects at the junctions of various cores in sandwich beams/panels is not understood completely, and a further study is needed.

The paper deals with the high-order modeling of the local stress concentrations at core junctions in sandwich beams under transverse loading. High-order modeling is a strong numerical tool, which allows studies of various geometries, along with gradual changes or inclined junctions, and material constitutions, linear and non-linear, of the sandwich beams/panels under small and large displacements. This will provide a full picture of the stress concentrations in the vicinity of the cores junctions and shed light on the failure mechanisms in these kinds of structures. A validation of the developed theory via experimental investigation of some representative sandwich beams subjected to three-point bending is also a subject of the paper.

Governing Equations

The nonlinear formulation consists of the derivation of the governing field equations. They are derived through the minimization of the total energy that consists of the internal energy and the external work. It reads as

$$\int_{t_1}^{t_2} \delta(U + V)\,\mathrm{d}t = 0 \tag{1}$$

where U and V are the internal and the external potential energy, respectively, and δ is the variation operator.

The first variation of the internal potential energy in terms of stresses and strains reads as

$$\delta U = \int_{V_t} (\sigma_{xxt}\delta\varepsilon_{xxt})\,\mathrm{d}v + \int_{V_b} (\sigma_{xxb}\delta\varepsilon_{xxb})\,\mathrm{d}v + \int_{V_c} (\tau_{xzc}\delta\gamma_{xzc} + \sigma_{zzc}\delta\varepsilon_{zzc})\,\mathrm{d}v \tag{2}$$

where σ_{xxj} and ε_{xxj}, $j = t, b$, are the longitudinal normal stresses and strains in the upper and the lower face sheet, respectively; τ_{xzc} and γ_{xzc} are the vertical shear stresses and shear strains in the core; σ_{zzc} and ε_{zzc} are the vertical normal stresses and strains in the vertical direction of the core; b_w and c are the width and the height of the core, respectively; w_j, $j = t, b$, are the vertical displacement of the upper and the lower face sheets, respectively (Fig 1a); and L is the span of the panel.

Received 9 December 2004; accepted for publication 16 May 2005.

*Associate Professor, Institute of Mechanical Engineering; eb@ime.aau.dk.

†Professor, Department of Civil Engineering; cvrfros@techunix.technion.ac.il.

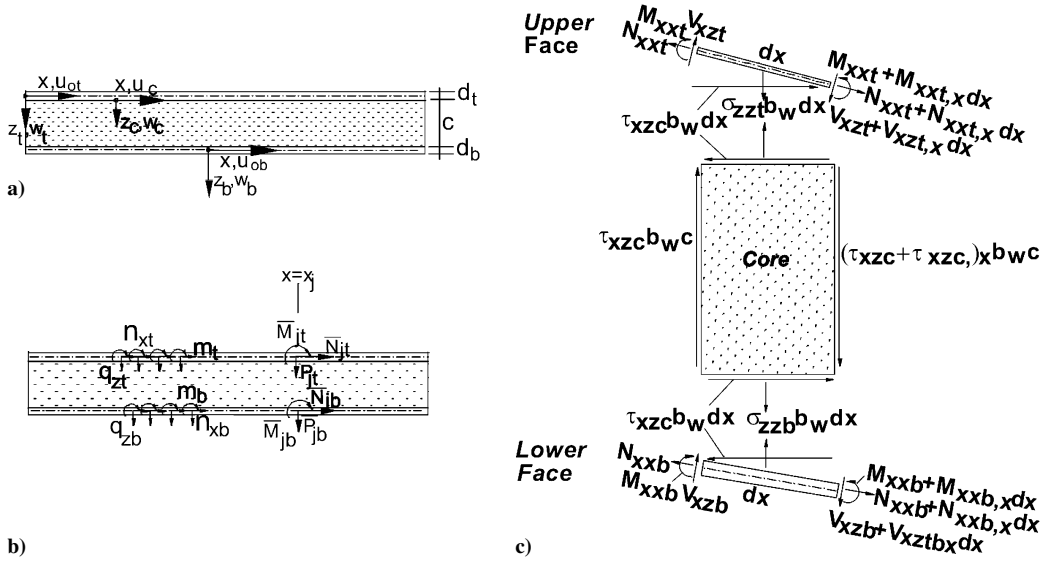

Fig. 1 Sandwich panel layout: a) geometry, b) external loads, and c) internal stress resultants.

The variation of the external work equals

$$\delta V = -\int_0^L \Big[n_{xt}\delta u_{ot} + n_{xb}\delta u_{ob} + q_{zt}\delta w_t + q_{zb}\delta w_b + m_t \delta w_{t,x} + m_b \delta w_{b,x} + \sum_{i=0}^{Nc} (\overline{N_{it}}\delta u_{ot} + \overline{P_{ib}}\delta u_{ob} + \overline{P_{it}}\delta w_t + \overline{P_{ib}}\delta w_b + \overline{M_{it}}\delta w_{t,x} + \overline{M_{ib}}\delta w_{b,x})\delta_D(x - x_{ci}) \Big] \mathrm{d}x \tag{3}$$

where u_{oj}, and w_j, $j = t, b$, are the displacements in the longitudinal and vertical directions, respectively, of the mid-plane of the face sheets; n_{xj} and q_{zj}, $j = t, b$, are the in-plane external loads in the longitudinal direction and the vertical distributed loads exerted on the upper and lower face sheets, respectively; m_j, $j = t, b$, are the distributed bending moments at the various face sheets; $\overline{N_{ji}}$, $\overline{P_{ji}}$, and $\overline{M_{ji}}$, $j = t, b$, are the external concentrated longitudinal and vertical load and bending moment, respectively, exerted at the upper and the lower face sheet at location $x = x_{ci}$; $\delta_D(x - x_{ci})$ is the delta of Dirac; N_c is the number of location with concentrated loads; and $w_{j,x}$, $j = t, b$, is the slope of the vertical displacement of the upper and lower face sheet, respectively. Sign convention for stresses, displacements, and loads appear in Fig. 1.

The kinematic relations with moderate displacements take the following form: For the face sheets, $j = t, b$,

$$\varepsilon_{xxj} = \varepsilon_{xxoj} + z_j \chi_{xxj} \tag{4}$$

where the midplane in-plane strains and curvatures are

$$\varepsilon_{xxoj} = u_{oj,x} + w_{j,x}^2/2, \qquad \chi_{xxj} = -w_{j,xx} \tag{5}$$

where ε_{xxo}, and χ_{xxj}, $j = t, b$, are the in-plane strains in the longitudinal direction of the midplane and the curvature of the upper and the lower face sheets, respectively; z_j is the vertical coordinate of each face sheet that is measured downward from the midplane of each face sheet (Fig. 1b); and $(\,)_{,x}$ denotes a derivative with respect to x.

For the core,

$$\gamma_c = u_{c,z} + w_{c,x}, \qquad \varepsilon_{zz} = w_{c,z} \tag{6}$$

where $u_c(x, , z_c)$ and $w_c(x, z_c)$ are the longitudinal and vertical deflections of the core, respectively, and z_c is the vertical coordinate of the core, measured downward from the upper interface (Fig. 2b).

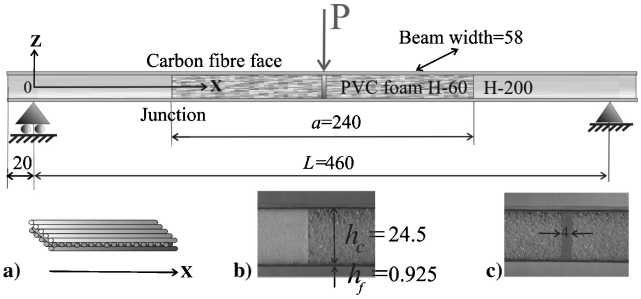

Fig. 2 Sandwich beam, dimensions in millimeters, a) with 3-layer laminate faces and two different core materials, b) zoom on the core junction, and c) central diaphragm.

The compatibility conditions at the upper and the lower face–core interface, $j = t, b$, are

$$u_c(x, Z_{cj}) = u_{oj} + \tfrac{1}{2}(-1)^k d_j w_{j,x}, \qquad w_c(x, z_{cj}) = w_j \tag{7}$$

where $k = 0$ when $j = t$ and $k = 1$ when $j = b$; $z_{ct} = 0$ at the upper interface and $z_{cb} = c$ at the lower interface (Fig. 1b); d_j, $j = t, b$, are the thickness of the upper and lower face sheets, and c is the height of the core after deformation (Fig. 1a).

The constitutive relations for each the laminated composite materials face sheets, $j = t, b$, are

$$N_{xxj}(x) = A_{11_j}\varepsilon_{xxoj} + B_{11_j}\chi_{xxj} \tag{8}$$

$$M_{xxj}(x) = B_{11_j}\varepsilon_{xxoj} + D_{11_j}\chi_{xxj} \tag{9}$$

where the strains and the curvatures are defined in Eq. (5) and A_{11j}, B_{11j}, and D_{11j} are the reduced stiffness coefficients of the laminated face sheets.

The governing equations are derived through substitution of the kinematic relations [Eqs. (4–6)] into the potential energy variation [see Eq. (2)] using the stress resultants in the face sheets (Fig. 1), the compatibility conditions and equilibrium requirements between the core and the face sheets at their interfaces [see Eq. (7)] along with constitutive relations for the face sheets [see Eqs. (8) and (9)], and an isotropic core. Hence, in their first order description, they are

$$\frac{\mathrm{d}}{\mathrm{d}x}N_{xxt}(x) = -n_{xt} - b_w\tau(x) \tag{10}$$

$$\frac{\mathrm{d}}{\mathrm{d}x}u_{ot}(x) = -\frac{1}{2}Dw_t(x)^2 - \frac{1}{2}\frac{2M_{xxt}(x)B_{11_t} - 2D_{11_t}N_{xxt}(x)}{-B_{11_t}^2 + D_{11_t}A_{11_t}} \tag{11}$$

$$\frac{\mathrm{d}}{\mathrm{d}x}V_{xzt}(x) = -\frac{b_w E_{zc} w_b(x)}{c} + \frac{b_w E_{zc} w_t(x)}{c} - \frac{1}{2}E_{zc} D[\tau(x)]\, b_w c - q_{zt} \tag{12}$$

$$\frac{\mathrm{d}}{\mathrm{d}x}M_{xxt}(x) = -\frac{1}{2}b_w d_t \tau(x) + m_t(x) - N_{xxt}(x) Dw_t(x) + V_{xzt}(x) \tag{13}$$

$$\frac{\mathrm{d}}{\mathrm{d}x}w_t(x) = Dw_t(x) \tag{14}$$

$$\frac{\mathrm{d}}{\mathrm{d}x}Dw_t(x) = -\frac{M_{xxt}(x)A_{11_t} - N_{xxt}(x)B_{11_t}}{-B_{11_t}^2 + D_{11_t}A_{11_t}} \tag{15}$$

$$\frac{\mathrm{d}}{\mathrm{d}x}N_{xxb}(x) = -n_{xb} + b_w \tau(x) \tag{16}$$

$$\frac{\mathrm{d}}{\mathrm{d}x}u_{ob}(x) = -\frac{1}{2}Dw_b(x)^2 - \frac{1}{2}\frac{2M_{xxt}(x)B_{11_b} - 2D_{11_b}N_{xxt(x)}}{-B_{11_b}^2 + D_{11_b}A_{11_b}} \tag{17}$$

$$\frac{\mathrm{d}}{\mathrm{d}x}V_{xzb}(x) = \frac{b_w E_{zc} w_b(x)}{c} - \frac{b_w E_{zc} w_t(x)}{c} - \frac{1}{2}E_{zc} D[\tau(x)] b_w c - q_{zb} \tag{18}$$

$$\frac{\mathrm{d}}{\mathrm{d}x}M_{xxb}(x) = -N_{xxb}(x) Dw_b(x) - \frac{1}{2}b_w d_b \tau(x) + m_b(x) + V_{xzb}(x) \tag{19}$$

$$\frac{\mathrm{d}}{\mathrm{d}x}w_b(x) = Dw_b(x) \tag{20}$$

$$\frac{\mathrm{d}}{\mathrm{d}x}Dw_b(x) = -\frac{M_{xxt}(x)A_{11_b} - N_{xxt}(x)B_{11_b}}{-B_{11_b}^2 + D_{11_b}A_{11_b}} \tag{21}$$

$$\frac{\mathrm{d}}{\mathrm{d}x}\tau(x) = E_{zc} D[\tau(x)] \tag{22}$$

$$\frac{\mathrm{d}[D(\tau(x)]}{\mathrm{d}x} = \left(-\frac{6d_t}{c^3} - \frac{6}{c^2}\right)Dw_t(x) + \left(-\frac{6}{c^2} - \frac{6d_b}{c^3}\right)Dw_b(x) + \frac{12u_{ot}(x)}{c^3} - \frac{12u_{ob}(x)}{c^3} + \frac{12\tau(x)}{c^2 G_{xzc}} \tag{23}$$

where N_{xxj} and M_{xxj}, $j = t, b$, are the in-plane and bending moment stress resultants of each face sheet; V_{xzj}, $j = t, b$, are the shear stress resultants in the upper and lower face sheets; $\tau(x)$ is the shear stress in the core; w_j and u_{oj}, $j = t, b$, are the vertical and horizontal midplane in-plane displacements of the face sheets; E_{zc} and G_{xzc} are the vertical modulus of elasticity and the shear modulus of the core; d_j, $j = t, b$, are the thickness of the upper and lower face sheets; and x is the longitudinal coordinate of the sandwich panel. See Fig. 1 for the adopted sign conventions and coordinates.

Note that the slope of the shear stress [see Eq. (22)] has been scaled with modulus of elasticity of the core, E_{zc}, to achieve an efficient numerical scheme.

The stress and displacement fields of the core are

$$\tau(x, z_c) = \tau(x) \tag{24}$$

$$\sigma_{zz}(x, z_c) = \left(\frac{c}{2} - z_c\right)E_{zc} D(\tau)(x) + \frac{[w_b(x) - w_t(x)]E_{zc}}{c} \tag{25}$$

$$w_c(x, z_c) = \left(\frac{1}{2}cz_c - \frac{1}{2}z_c^2\right)D(\tau)(x) + \left(1 - \frac{z_c}{c}\right)w_t(x) + \frac{z_c w_b(x)}{c} \tag{26}$$

$$u_c(x, z_c) = \frac{z_c \tau(x)}{G_{xzc}} + u_{ot}(x) + \left(-z_c + \frac{1}{2}\frac{z_c^2}{c} - \frac{1}{2}d_t\right)Dw_t(x) - \frac{1}{2}\frac{z_c^2 Dw_b(x)}{c} + \left(-\frac{1}{4}cz_c^3 + \frac{1}{6}z_c\right)\frac{\mathrm{d}}{\mathrm{d}x}D(\tau)(x) \tag{27}$$

where $\tau(x, z_c)$ and $\sigma_{zz}(x, z_c)$ are the core shear and the transverse normal stresses $w_c(x, z_c)$ and $u_c(x, z_c)$ are the vertical and in-plane displacements of the core, respectively, and, finally, z_c is the vertical coordinate of the core measured from the upper face–core interface. See Fig. 1 for sign conventions. The complete derivation of Eqs. (10–28) may be found by Frostig and Baruch in Ref. 8.

The continuity conditions between the various regions, at $x = x_k$, follow.

For each of the face sheets, $j = t, b$,

$$u_{oj}^{(-)} = u_{oj}^{(+)}, \qquad w_j^{(-)} = w_j^{(+)}, \qquad w_{j,x}^{(-)} = w_{j,x}^{(+)} \tag{28}$$

$$N_{xxj}^{(-)} - N_{xxj}^{(+)} - \bar{N}_i = 0, \qquad -M_{xxj}^{(-)} + M_{xxj}^{(+)} - \bar{M}_i = 0$$

$$V_{xzj}^{(-)} - V_{xzj}^{(+)} - \bar{P}_i = 0 \tag{29}$$

where $(-)$ and $(+)$ refer to left and right of joint, respectively.

For the core,

$$\tau^{(-)} - \tau^{(+)} = 0, \qquad w_c\left(x_k^{(-)}, z_c\right) = w_c\left(x_k^{(+)}, z_c\right) \tag{30}$$

Please notice that the displacement conditions in the core [Eqs. (30)] require full compatibility through the depth of the core at the joint. It is equivalent [see Eq. (26)] to the following requirement imposed on the slope of the shear stresses in the core as follows:

$$D\left(\tau^{(-)}\right)(x_k) = D\left(\tau^{(+)}\right)(x_k) \tag{31}$$

The experimental study is presented next.

II. Experimental Study

The experimental study concerned a sandwich beam shown schematically in Fig. 2. The beam consists of composite laminated faces with a symmetrical layup of 0/90/0 deg (Fig. 2a). The face laminates are made of carbon fiber prepregs (SP Systems[9]) and have been manufactured by means of a manual layout with a subsequent vacuum bagging at the prescribed temperature and pressure.[10] The tensile stiffness of the composite laminate has been measured experimentally by means of modal analysis[11] and standard tensile test.[12] In the first case, the first three eigenfrequencies of the cantilever beam (cut from the face laminate) were excited and measured, and the integral modulus of elasticity of the composite has been calculated as an average of these measurements. In the second case, the standard routine of recording the load vs deformation has been carried out, and subsequent calculation of the modulus of elasticity as a slope of this dependence yields the equivalent modulus of elasticity of the face. Both methods yield the same equivalent modulus of elasticity for the beam face, equal to 83.3 GPa with an error that did not exceed 4%. The mechanical properties of a single lamina appear in Table 1 according to Ref. 10. Two types of core materials are used in the investigated beams: a compliant core H-60 and a stiff one H-200 (DIAB Group[13]) with the respective densities of 60 and 200 kg/m^3. Their mechanical characteristics are indicated in Table 1. The stiff core constituted the ends of the specimens and the compliant core their central part. A zoom on the core junction is presented

Table 1 Elastic properties of the beam constituents

Property	Faces: carbon fiber laminate	Compliant core: PVC foam H60	Stiff core: PVC foam H200
Modulus of elasticity, MPa	83,300	60	310
Shear modulus, MPa	——	22	90
Yield strength, MPa	1190[a]		
	2840[b]	0.8[c]	4.5[c]
	12[d]	1.4[e]	4.8[e]
Shear yield strength, MPa	——	0.7	3.3

[a]Compression along the fiber. [b]Tension along the fiber. [c]Compression. [d]Across fiber. [e]Tension.

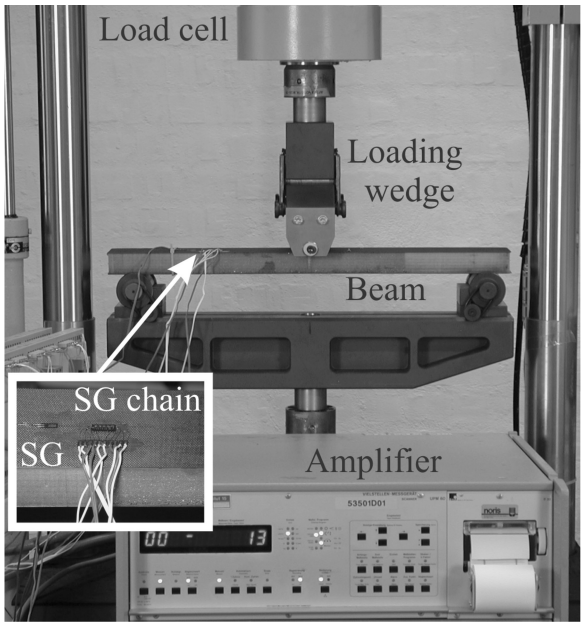

Fig. 3 Experimental setup for three-point bending of sandwich beam.

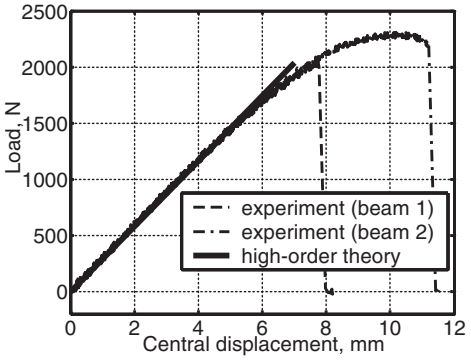

Fig. 4 Central load vs central displacement dependence for beams loaded in three-point bending.

in Fig. 2b. All of the components of the panel are joined using an epoxy resin, Araldite® 2022 (Huntsman Advanced Materials).

Three beam specimens were manufactured: two for ultimate loading up to the failure and one for the study of the static deformation behavior. For the latter purpose, the third beam had a strain gauge chain located on the face across the core junction, as shown in zoom in Fig. 3, and a single strain gauge positioned 15 mm to the left from the junction.

A three-point bending scheme[14] as shown in Fig. 2 has been chosen for an experimental investigation of the sandwich beams with junctions. To avoid localized effects in the center of the specimens, a rigid diaphragm has been included. The diaphragm with the thickness of 4 mm (Fig. 2c) has been manufactured in a separate step mold from the same adhesive that has been used for gluing the sandwich components and, subsequently, has been glued into the a rectangular groove machined in the center of the beam core before attaching the second face.

The testing rig is built on the basis of a servohydraulic machine,[15] SCHENK Hydropuls® PSB, and includes a computerized data acquisition (Fig. 3). The testing rig operated in a displacement control mode with the accuracy of the appropriate load measurement of better than 0.2%.

Beams 1 and 2 have been tested up to failure. Load vs central displacement dependences of these beams are linear up to 1.5 kN and are shown in Fig. 4. The maximum critical loads for the beams 1 and 2 are 2.06 and 2.31 kN, respectively. The third beam has been loaded only in the linear region, and its load–displacement curve in this range is similar to those of the beams that have been tested up to failure. Notice a good coincidence between the analytical high-order modeling and experimentally recorded data in Fig. 4.

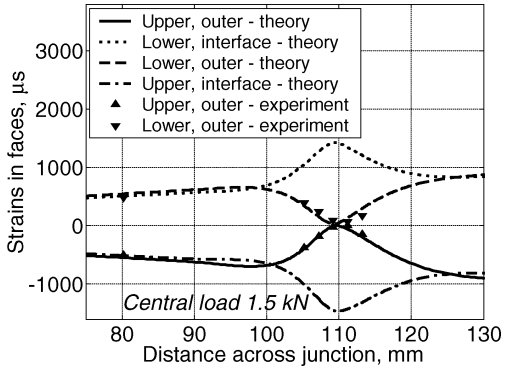

Fig. 5 Distributions of strains in sandwich faces.

Figure 5 shows strain distributions in the faces of the sandwich beam for the central load of 1.5 kN. They are calculated numerically along at the outer fibers of each face of the beam, that is, outer surfaces and face–core interfaces. The upper face is generally in compression, whereas the lower one is in tension. (Notice that in Fig. 5 and as well be show subsequently the distance across the junction is referred to according to the coordinate system of Fig. 2.) The strains at the outer surfaces of the faces have been measured, and these data are also presented in Fig. 5. The heights of the triangles, which represent the experimental data, correspond to the absolute error of the strain measurements, which is equal to $\pm 30 \times 10^{-6}$. As expected, the strains (and stresses) in the faces of the beam subjected to the central load increased linearly from zero at the edges of the beam up to a maximum value in the beam center. If one follows traditional conviction, then in the vicinity of a junction one should expect strains of -720×10^{-6} and $+720 \times 10^{-6}$ in the upper and lower faces, respectively, and these strains should be almost constant through the thickness of each face. This is not the reality though, when two different core materials are adjoined in the sandwich core in the trimaterial corners. First, a local effect will manifests itself in an additional local bending moment in the beam faces, which leads to a significant variation of the stresses through-the-thickness of the face sheets. For this particular beam, the strains at the outer surfaces of the face sheet plummeted up to zero, as shown both theoretically and experimentally. At the same time, the face strains increase almost to twice at the face–core interface, and they have reached a value of $\pm 1400 \times 10^{-6}$, which corresponds to stresses of ± 180 MPa in the outer layers of the face lamina. Generally such local stress concentrations may cause a failure of the face sheet, especially when it is made of anisotropic materials, which exhibit different strength properties in tension and compression (Table 1).

III. Discussion

Although local effects in the face sheets in the vicinity of the junctions are very pronounced, most probably it is not in the faces one should expect a failure of sandwich structure, but in the adjacent cores. The sandwich cores are the weakest components of the structure, and therefore, it is of interest to uncover the nature of the local effects there. Figure 6 shows the distributions of the strains in the core across the core junction. Here one can see that the shear stress τ_c, which is constant through the thickness of the core in the high-order model, varies longitudinally across the junction: τ_c achieves a value of 0.6 MPa in the stiffer core for the average level of 0.5 MPa through the whole panel and far away of the junction. What is most important is the rise of the transverse normal stresses σ_c, which are usually ignored in a sandwich panel with a homogenous core far from the vicinity of localized loads and supports. It is important that a mere existence of the core junction gives a rise to σ_c, which exactly at the junction attains substantial values of 1.3 and 0.6 MPa in the stiff H-200 and compliant H-60 cores, respectively. The normal stresses in the cores vary through-the-thickness of the core. They

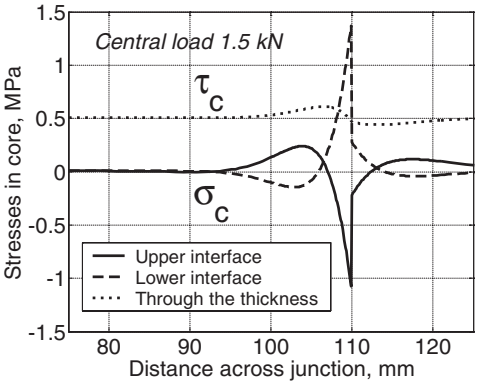

Fig. 6 Stress distributions in core of sandwich beam modeled with high-order theory.

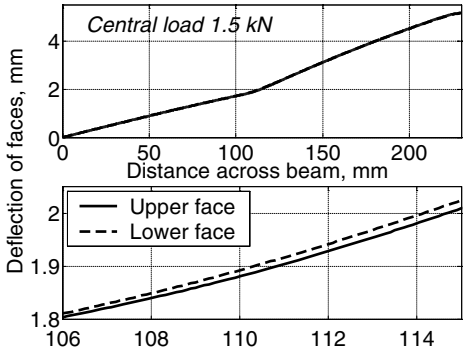

Fig. 7 Deflection of beam faces modeled with high-order theory.

are compressive at the upper face–core interface and tensile at the lower one. Obviously, the principle stress in the compliant core may easily exceed the yield strength of the core; compare strength characteristics of H-60 with the data from Fig. 6. Then a failure of the compliant core may happen due to compression (at upper interface) or tension (at lower interface) in the trilateral corners of the junctions. To be exact, here high levels of the locally induced normal stresses are quite dangerous because a possible failure of the core may accompanied by the delamination of the face and core, which may develop into a collapse of the whole structure.

Findings of Fig. 6 are substantiated by results presented in Fig. 7, where deflections of the upper and lower faces of the sandwich beam are calculated. Note the bend of the face sheets precisely at the core junction. This is an unambiguous sign of the drastic change of the shear deformation from one type of core to another, and this is a clear evidence of the local effects at the junction. Overall, there is no substantial difference in the deflections of the faces except at a zone of the junction, which is shown in the zoom plot in Fig. 7. One can see that the displacement of the lower face is about 0.02 mm larger than that of the upper face, and this is a confirmation of a transverse "opening" of the beam at the core junction.

IV. Conclusions

Sandwich panels with junctions of different core materials loaded by transverse loads are considered. It is shown, with the help of a high-order model, that the local effects arise in all sandwich constituents in the vicinity of junctions. The zone with the local effects extends left and right of the junction, and it is of the order of the core thickness. The local stress concentrations are observed as additional bending stresses in the faces, variation of the shear stresses, as well as an appearance of the normal through-the-thickness stresses in the adjacent cores. Experimental investigation of the sandwich beams loaded in the three-point bending confirmed the findings of the high-order modeling.

The numerical study has revealed that the intensity of the local effects is proportional to the discrepancy of the elastic properties of the adjoined cores. Weaker and thinner faces also amplify the degree of the locally induced stresses. The first fact indicates a possibility of design optimization of beams with core junctions by means of smoothing transition zones via inserting, for example, intermediate patch of the core between the compliant and stiff cores. The second fact suggests a local reinforcement of the face sheets at core junctions to suppress their unwanted local bending.

The rise of the normal local stresses in the weakest core at the trimaterial corners of the junctions is an important parameter of the stress state of the sandwich panel when subjected to transverse loading. If this stress reaches the strength limit of the material, it might trigger the failure of the whole sandwich structure. Therefore, detailed estimations of the locally induced stresses in all sandwich components at core junctions should be an obligatory phase in the design of sandwich beams, panels, and shells.

Acknowledgment

The support of DIAB ApS, Denmark, for supplying the PVC foam cores for the experimental investigations is gratefully appreciated.

References

[1]Zenkert, D. (ed.), *The Handbook of Sandwich Construction*, EMAS Pub., London, 1997, Chaps. 9, 10.

[2]Zenkert, D., *An Introduction to Sandwich Construction*, EMAS Pub., London, 1995, Chaps. 3,4,14.

[3]Allen, H. G., *Analysis and Design of Structural Sandwich Panels*, Pergamon, Oxford, 1969, Chaps. 5,6,9.

[4]Frostig, Y., and Baruch, M., "Bending of Sandwich Beams with Transversely Flexible Core," *AIAA Journal*, Vol. 28, No. 3, 1990, pp. 523–531.

[5]Frostig, Y., Baruch, M., Vilnay, O., and Sheinman, I., "A High Order Theory for the Bending of Sandwich Beams with a Flexible Core," *Journal of ASCE, EM Division*, Vol. 118, No. 5, 1992, pp. 1026–1043.

[6]Skvortsov, V., and Thomsen, O. T., "Analytical Estimates for the Stresses in Face Sheets of Sandwich Panels at the Junctions Between Different Core Materials," *Proceedings of the 6-th International Conference on Sandwich Structures*, edited by J. Vinson, Y. Rajapakse, and L. Carlsson, CRC Press, New York, 2003, pp. 501–509.

[7]Bozhevolnaya, E., Thomsen, O. T., Kildegaard, A., and Skvortsov, V., "Local Effects across Core Junctions in Sandwich Panels," *Composite Part B: Engineering*, Vol. 34, No. 6, 2003, pp. 509–517.

[8]Frostig, Y., and Baruch, M., "Buckling of Simply-Supported Sandwich Beams with Transversely Flexible Core—A High Order Theory," *Journal of ASCE, EM Division*, Vol. 119, No. 3, 1993, pp. 476–495.

[9]Product Catalog, *SP Systems Product Catalog* [online database], URL: http://www.spsystems.com/solutions/general_pdfs/UK_2004_PC_v1.pdf [cited 25 Oct. 2004].

[10]"Prepregs and Adhesive Films," *SP Systems Product Selector Guide* [online database], URL: http://www.spsystems.com/solutions/solutions_pdfs/pdfs_productdatasheets/prepreg/SE_84.pdf [cited 25 Oct. 2004].

[11]Ewins, D. J., *Modal Testing: Theory and Practice*, Research Studies Press, Ltd., Letchworth, England, U.K., 1985, p. 269.

[12]"Standard Test Method for Young's Modulus, Tangent Modulus, and Chord Modulus," Annual Book of American Society for Testing and Materials Standards, Rept. E111-82, ASTM, West Conshohocken, PA, Aug. 1982 (reapproved 1988).

[13]"Strutural Foam Cores," *DIAB Products* [online database], URL: http://www.diabgroup.com/europe/products /e_prods_2.html [cited 25 Oct. 2004].

[14]"Standard Test Method for Flexural Properties of Sandwich Constructions," Annual Book of American Society for Testing and Materials Standards, Rept. C393-00, ASTM, West Conshohocken, PA, April 2000.

[15]"SCHENK Hydropuls® System," Instruction Manual, Carl Schenk AG, Darmstadt, Denmark, 1986 (updated 2001).